

A vortex-dipole sheet model for a wake

Robert Krasny

Department of Mathematics, University of Michigan, Ann Arbor, Michigan 48109-1003

(Received 10 August 1988; accepted 5 October 1988)

A vortex model for a free shear layer with a wake component is proposed. The layer is represented by a curve which supports both a vortex sheet and a vortex-dipole sheet. The vortex sheet yields a monotonic velocity profile that connects the outer flows on either side of the shear layer. The vortex-dipole sheet captures the effect of oppositely signed vorticity that is present in the wake due to boundary layers upstream from the separation point. The equations governing a vortex-dipole sheet are given and a temporal instability calculation for a free sinusoidal wake shows the development of a vortex street.

The purpose of this Letter is to propose a vortex model for a wake that uses vortex dipoles as well as point vortices to represent the vorticity field. To avoid additional complications, this discussion will be restricted to two-dimensional flow, periodic in the streamwise direction.

Consider a free shear layer with a wake component, such as that which might form behind a solid body in a streaming flow. Suppose that the shear layer is parallel and that locally it consists of two components as shown in Fig. 1. The first ("shear") component is antisymmetric about the layer's centerline $y = 0$. It has a monotonic velocity profile which converges to a uniform stream as $y \rightarrow \pm \infty$. The second ("wake") component is symmetric about the centerline and it corresponds to the velocity deficit in the free shear layer. The wake component results from the boundary layers along the body, upstream from the separation point. Both the shear and the wake components contribute vorticity to the flow field. While the shear component contains vorticity of one sign, the wake component guarantees that oppositely signed vorticity exists in the shear layer for some distance downstream from the separation point.¹ The wake component has an important effect upon the stability characteristics of the shear layer.²

Computational vortex methods approximate a given vorticity field by a collection of smoothed point vortices, each having vorticity of one sign.^{3,4} Convergence for a general class of flows has been proven, provided that the point vortex singularity is appropriately smoothed.⁵ In view of the preceding remarks, it is natural to also consider using vortex dipoles, each possessing vorticity of both signs, in order to approximate the wake component of a free shear layer.⁶

One approach taken by previous investigators has been to represent the vorticity in the wake by either a pair of vortex sheets⁷⁻⁹ or layers of constant vorticity.¹⁰ Consider instead a model in which the free shear layer is represented by a single curve that supports both a vortex sheet and a vortex-dipole sheet. The vortex sheet represents the antisymmetric shear component of the velocity and the vortex-dipole sheet represents the symmetric wake component. An individual vortex dipole results from taking the directional derivative of a point vortex; in particular, it has a position, a magnitude, and a direction.¹¹ Just as the vortex sheet may be viewed as a collection of point vortices lying on a curve, the vortex-dipole sheet is defined by distributing vortex dipoles along a curve. In the proposed model for a free shear layer with a

wake component, each vortex dipole is the normal derivative of a point vortex on the curve. Thus the self-induced velocity of the vortex dipole is tangential to the curve.

The vortex sheet has a self-induced velocity given by the Birkhoff-Rott equation. This equation can be generalized to include the velocity component induced by a vortex-dipole sheet. The singular integrals that appear in the resulting evolution equation are dealt with by introducing a smoothing parameter.¹² In the remainder of this Letter, we present the equations governing the evolution of a vortex-dipole sheet and then show calculations for a simple test case, the free sinusoidal wake.

The curve that represents the wake centerline has coordinate functions $x(a,t)$ and $y(a,t)$. The variable a is a Lagrangian parameter along the curve. Let $G(x,y)$ be the Green's function for the Laplace equation in two dimensions. The circulation density along the curve is defined by a function $\sigma(a)$ and the vortex-dipole distribution is given by a vector-valued function $\mathbf{D}(a,t)$. The streamfunction at the field point (x,y) is expressed as

$$\psi(x,y,t) = \int G\sigma da - \int \nabla G \cdot \mathbf{D} da.$$

In this equation, G and its gradient ∇G are evaluated at $(x - x(a,t), y - y(a,t))$ and the integration is performed with respect to the Lagrangian variable. The first integral accounts for the vortex sheet and the second integral for the vortex-dipole sheet. Velocity components are defined as usual for incompressible flow: $u = \psi_y$, $v = -\psi_x$. The necessary partial derivatives of ψ are obtained by analytically differen-

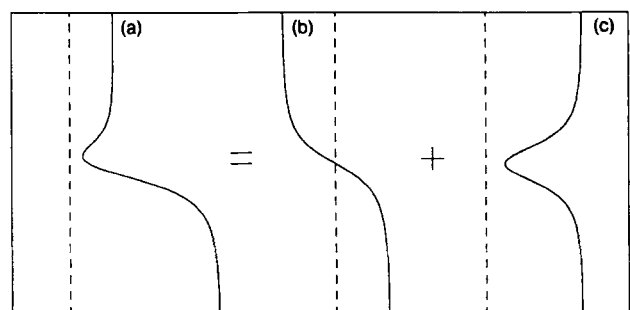


FIG. 1. Schematic diagram of a local velocity profile. (a) Free shear layer; (b) shear component; and (c) wake component.

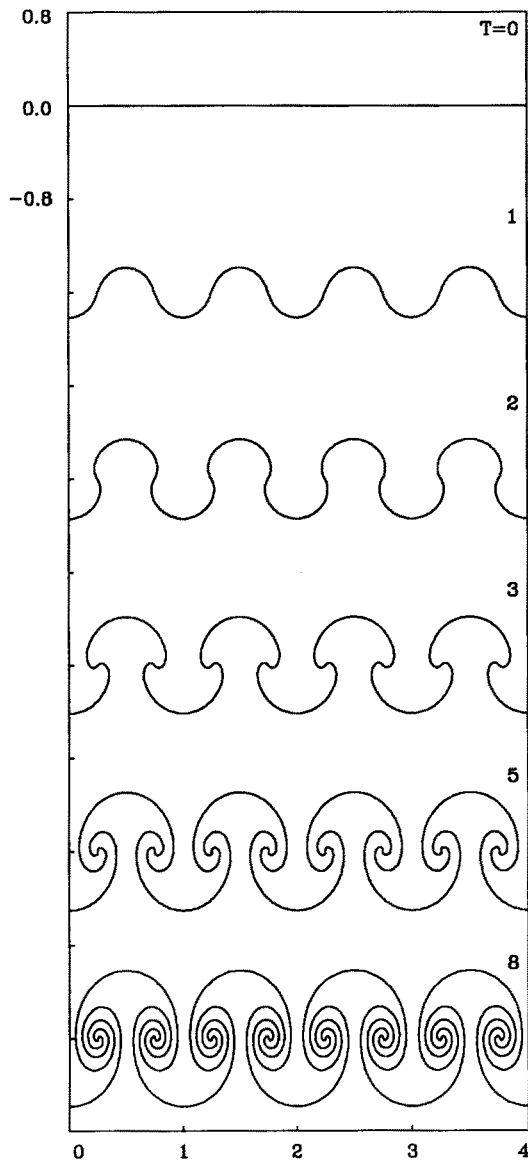


FIG. 2. Time evolution with a zero vortex-dipole distribution ($D = 0$). The pair of counter-rotating vortices in each wavelength remains on the line $y = 0$.

tiating G and ∇G under the integral sign. Evaluating the integrals on the curve yields the equations of motion $x_i = u$, $y_i = v$. Velocity derivatives $\nabla \mathbf{u}$ are also defined by repeated differentiation of $G(x, y)$ under the integral sign and then evaluating the resulting expressions on the curve.¹³ The vortex-dipole distribution evolves according to $\mathbf{D}_t = -\nabla \mathbf{u}^T \cdot \mathbf{D}$, the equation satisfied by the vorticity gradient in two-dimensional incompressible inviscid flow.

In the calculations, a smoothing parameter δ is introduced and the singular Green's function is replaced by the following periodic regular approximation¹⁴:

$$G(x, y; \delta) = (-1/4\pi) \log(\cosh 2\pi y - \cos 2\pi x + \delta^2).$$

The value $\delta = 0.5$ was used to obtain the results shown below. The curve parameter a is discretized and the integrals are approximated by the trapezoidal rule. Each discrete vortex element now corresponds to a smoothed point-vortex/vortex-dipole combination. This leads to a system of ordi-

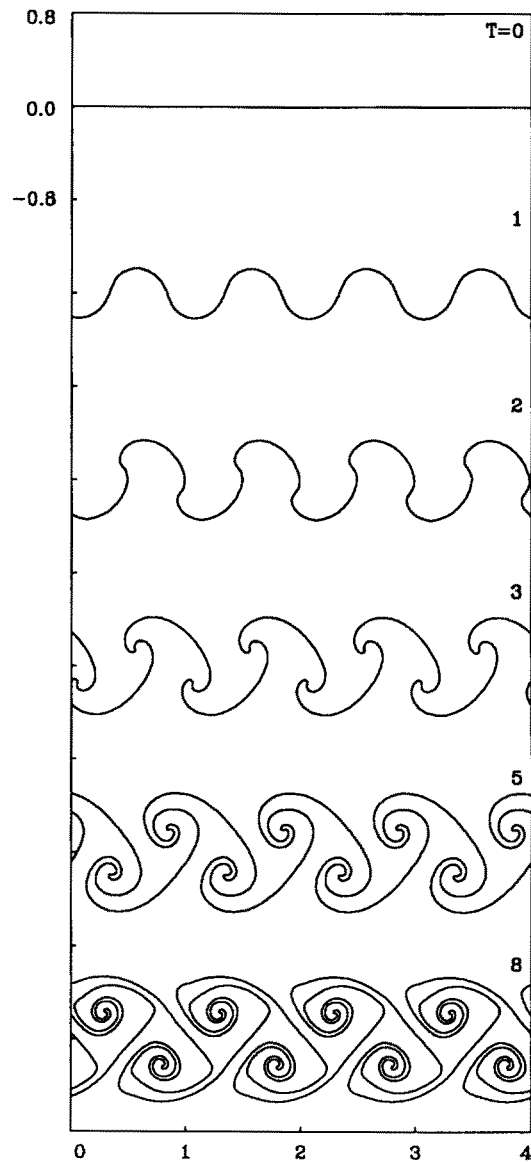


FIG. 3. Time evolution with a nonzero vortex-dipole distribution ($D = 0.025$). The vortices form a vortex street.

nary differential equations for the point positions and the dipole distribution. The system was integrated forward in time and a point insertion technique was used to maintain resolution.¹²

Initial conditions were chosen to simulate a free sinusoidal wake. The curve is initially flat [$x(a, 0) = a$, $y(a, 0) = 0$] but has circulation density $\sigma(a) = \sin 2\pi a$. The vortex dipoles are aligned vertically [$\mathbf{D}(a, 0) = D \cdot (0, 1)$] and have constant magnitude D . Calculations using the values $D = 0$ and $D = 0.025$ are shown in Figs. 2 and 3, respectively. Four periods of the curve are plotted at various times in these figures.

Both curves deform similarly for short times under the influence of the circulation distribution. The curve possesses two inflection points in each wavelength that later evolve into centers of counter-rotating vortices. When the vortex-dipole distribution is zero (Fig. 2), the vortices remain on the line $y = 0$, as observed for stratified flow in the Boussin-

esq limit.¹⁵ Note that the vortices entrain fluid equally from both sides of the layer.

When the vortex-dipole distribution is nonzero (Fig. 3), the symmetry is upset and alternate vortices are staggered on either side of the line $y = 0$. The resulting pattern resembles the flow visualization of a laminar vortex street behind an oscillating body.^{16,17} Note that here the counterclockwise rotating vortices (which all lie above $y = 0$) entrain more fluid from the upper stream than from the lower stream. The situation is reversed for the clockwise-rotating vortices. It was also observed that a pure vortex sheet (i.e., $D = 0$) can form a vortex street when its initial shape is sinusoidally perturbed. In this case, however, the staggered vortices entrain fluid symmetrically; such results will be presented elsewhere. The particular initial conditions used here were chosen in order to demonstrate and emphasize the effect of the vortex-dipole distribution.

Further investigation of the vortex-dipole sheet model is under way and several questions need to be addressed in the future. For example, does the limit $\delta \rightarrow 0$ for a vortex-dipole sheet yield a weak solution of the Euler equations?¹⁸ Given a general vorticity field, what are the relative merits of computing with vortex dipoles or with point vortices of opposite sign? Can the model be extended to account for cancellation of oppositely signed vorticity? Application of the vortex-dipole sheet model to spatial instability and unsteady separation is also a future goal.

ACKNOWLEDGMENTS

The author would like to acknowledge helpful conversation with C. Börgers, D. Papageorgiou, and G. Winckelmanns.

This work was supported by the National Science Foundation Grant No. DMS-8801991.

- ¹D. B. Lang, Ph.D. thesis, California Institute of Technology, 1985.
- ²M. M. Koochesfahani and C. E. Frierler, AIAA Paper No. 87-0047, 1987.
- ³A. J. Chorin, *J. Fluid Mech.* **57**, 785 (1973).
- ⁴A. Leonard, *J. Comput. Phys.* **37**, 289 (1980).
- ⁵C. Anderson and C. Greengard, *SIAM J. Numer. Anal.* **22**, 413 (1985).
- ⁶M. F. McCracken and C. S. Peskin, *J. Comput. Phys.* **35**, 183 (1980).
- ⁷C. Börgers, *Math. Comp.* (in press).
- ⁸W. T. Ashurst and E. Meiburg, *J. Fluid Mech.* **189**, 87 (1988).
- ⁹H. Aref and E. D. Siggia, *J. Fluid Mech.* **109**, 435 (1981).
- ¹⁰C. Pozrikidis and J. J. L. Higdon, *Phys. Fluids* **30**, 2965 (1987).
- ¹¹L. M. Milne-Thomson, *Theoretical Hydrodynamics* (MacMillan, London, 1968), p. 361.
- ¹²R. Krasny, *J. Fluid Mech.* **184**, 123 (1987).
- ¹³C. Anderson, *J. Comput. Phys.* **61**, 417 (1985).
- ¹⁴R. Krasny, *J. Comput. Phys.* **65**, 292 (1986).
- ¹⁵G. Tryggvason, *J. Comput. Phys.* **75**, 253 (1988).
- ¹⁶M. Van Dyke, *An Album of Fluid Motion* (Parabolic, Stanford, CA, 1982), p. 57.
- ¹⁷M. M. Zdravkovich, *J. Fluid Mech.* **37**, 491 (1969).
- ¹⁸R. J. DiPerna and A. Majda, *Commun. Pure Appl. Math.* **40**, 301 (1987).

Correspondence principle for turbulence: Application to the Chicago experiments on high Rayleigh number Bénard convection

Victor Yakhot

Program in Applied and Computational Mathematics, Princeton University, Princeton, New Jersey 08544

(Received 13 September 1988; accepted 16 November 1988)

The correspondence principle postulated for the description of hydrodynamic turbulence [Phys. Rev. Lett. **57**, 1722 (1986)] combined with the theory of thermal boundary layer [B. Castaing *et al.* (private communication)] is applied to high Rayleigh number convection in a Bénard cell. Quantitative interpretation of recent experimental data [B. Castaing *et al.* (private communication)] is presented. The predicted intermittency exponent following from comparison of the theory with experiment is $0.175 < \mu < 0.275$. A crucial experimental test of the renormalization group theory of turbulence is proposed.

Recent experiments on high Rayleigh number thermal convection conducted at the University of Chicago revealed some new and rather unexpected results contradicting conventional (classical) ideas about turbulence in the Bénard cell.¹ The extraordinary quality of the experiments makes thermal turbulence in the Bénard cell an excellent, perhaps unique, system on which our theoretical understanding of the fine details of turbulence can be tested. The most important results of the Chicago experiments concern dependencies of different mean properties of the flow (helium gas with Prandtl number $Pr = 0.7$) on the Rayleigh number defined as $Ra = \alpha g \Delta L^3 / \kappa_0 \nu_0$, where g is the acceleration of gravity,

α is the volume expansion coefficient, Δ is the temperature difference between the top and bottom plates of the cell, L is the height of the cell, and κ_0 and ν_0 are the molecular thermal diffusivity and viscosity coefficients, respectively. The experimental results in the high Rayleigh number ($Ra \geq 10^7$) regime are (i) Nusselt number $Nu = HL / \kappa_0 \Delta$, where H is the constant heat flux, varies with Ra as

$$Nu \propto Ra^\beta, \quad \beta = 0.282 \pm 0.006; \quad (1)$$

(ii) mean temperature fluctuation measured at the center of the cell: